JOURNAL OF NANO- AND ELECTRONIC PHYSICS
Vol. **6** No 4, 04030(7pp) (2014)

ЖУРНАЛ НАНО- ТА ЕЛЕКТРОННОЇ ФІЗИКИ
Том **6** № 4, 04030(7cc) (2014)

Control of Morphology and Properties of Zinc Oxide Nanostructures Manufactured by Pulsed Electrochemical Deposition

N.P. Klochko[1,*], G.S. Khrypunov[1], Y.O. Myagchenko[2], E.E. Melnychuk[2], V.R. Kopach[1], K.S. Klepikova[1], V.M. Lyubov[1], A.V. Kopach[1]

[1] *National Technical University "Kharkiv Polytechnic Institute", 21, Frunze Str., 61002 Kharkiv, Ukraine*
[2] *National Taras Shevchenko University, 60, Volodymyrska Str., 01033 Kyiv, Ukraine*

(Received 02 September 2014; published online 29 November 2014)

In this paper we study ways to control the morphology and properties of zinc oxide nanostructures, which are produced by pulsed electrochemical deposition. The effect of mixing of electrolyte, changes in the shape of rectangular pulses of the cathode-substrate potential, as well as the electrolyte composition and duration of the pulsed electrodeposition process on the morphology, crystal structure and optical properties of nanostructured ZnO arrays has been demonstrated. The reasons for the formation by pulsed cathodic electrodeposition without introducing of surfactant growth modifiers into the electrolyte of ZnO arrays, consisting of regular hexagonal nanoplates and their stacks with vertical or horizontal arrangement with respect to the substrates, layers of paraboloid ZnO nanostructures, as well as one-dimensional arrays of zinc oxide, oriented perpendicular to the substrate were analyzed. It was demonstrated by the atomic force microscopy the manufacture of these nanostructured zinc oxide arrays. By the X-ray diffraction and optical spectroscopy the structure and properties of ZnO nanostructures fabricated by pulsed electrochemical deposition were studied.

Keywords: Zinc oxide, Pulse electrodeposition, Nanostructure, Atomic force microscopy.

PACS numbers: 61.46.Km, 68.37.Ps

1. INTRODUCTION

Interest in synthesis and application of nanostructured materials, namely, nanowires, nanoribbons, nanohelixes, nanorods, nanotetrapods, hierarchical nanostructures, nanotubes, lamellar and cone-shaped nanostructured arrays, rapidly increases in recent years due to the unique electronic, optical and optoelectronic properties of these objects. Nanostructured zinc oxide (ZnO) is especially important technological material because of availability, low cost, chemical stability, biocompatibility and unique combination of chemical and physical properties. In particular, ZnO nanostructures are used in the designs of gas sensors, supercapacitors, solid-state, hybrid and organic solar cells, light emitting diodes, tools for biochemical sensing, ultraviolet lasers, high-performance nanosensors, piezoelectric nanogenerators, short-wave light emitting optoelectronic nanodevices [1-13]. During the last decades, electrochemical deposition became an important method for the production of nanostructured ZnO arrays due to manufacturability, possibility of deposition on large areas, cost efficiency, good quality of the films and low synthesis temperatures in comparison with other methods. As the authors of the works [1, 5-11, 13] indicate, morphology and thickness of arrays, as well as their crystal structure and physical and chemical properties, can be easily controlled in this method by setting the deposition parameters, such as current density or electrode potential, composition and temperature of the solution, electrodeposition time. The authors of modern detailed reviews on electrochemical deposition of ZnO [1, 6] note that arrays of ZnO nanorods or nanowires, which are vertically oriented to the substrate, can be produced by the direct-current electrochemical method and that morphology of ZnO is utterly sensitive to the synthesis conditions. In all cases of electrochemical synthesis of ZnO nanostructures, correlation between generation rate of hydroxyl groups (OH^-) on the cathode and diffusion rate of zinc ions (Zn^{2+}) toward the cathode is accepted to be the most important factor which influences their morphology, structure and properties [1-6]. Therefore, at direct-current electrical deposition, geometry of one-dimensional (1D) arrays of zinc oxide is governed [1, 6] by using as electrolytes of more or less concentrated solutions of zinc salts, whose anions (chloride, sulphate, nitrate or acetate) possess or not a specific adsorption on certain faces of ZnO crystal lattice and also can or cannot be restored on the cathode with the formation of OH^- groups. Moreover, changes in the electrolyte temperature, cathode current density or cathode-substrate potential are used as the growth modifiers of zinc oxide arrays. For a radical change in the morphology of nanostructures, for example, in order to obtain nanolamellar arrays with vertical or horizontal arrangement of nanoplates or arrays of cone-shaped nanostructures, surfactant chlorides or organic additives (ethylenediamine, hexamethylenetetramine), which block diffusion of zinc ions to certain faces of growing ZnO crystals, are introduced into electrolytes at direct-current electrodeposition [1, 5-6]. We note that surfactant additives during the electrodeposition process inevitably introduce impurities into ZnO nanostructures which can negatively influence the quality of devices manufactured on their basis.

The process of pulsed electrochemical deposition, in contrast to the direct-current one, is characterized by a number of additional parameters, using which it is possible to affect the morphology, structure and properties of ZnO without recourse to use of surfactant additives in electrolyte.

* klochko_np@mail.ru

The same technique has been already demonstrated by the authors of [14] and in our works on the pulsed electrodeposition of nanostructured arrays of zinc oxide [7, 8, 10, 11]. Moreover, analysis of the literature has shown that influence of mixing during electrodeposition of ZnO is out of interest, although the authors of [1, 15] have described electrodeposition of 1D arrays of zinc oxide on a rotating disc electrode. It is not taken into account the obvious fact that convection radically changes the mass transfer conditions in electrolyte, and, on the other hand, correlations between generation rate of hydroxyl groups on the cathode and diffusion rate of zinc ions determine the morphology of electrodeposited arrays. In order to remove the existing gap in investigations, in the given work we demonstrate the influence of electrolyte mixing, change in the shape of rectangular pulses of the cathode-substrate potential and also composition of electrolyte and duration of the pulsed electrodeposition process on the morphology, crystal structure and optical properties of nanostructured ZnO arrays. We demonstrate the possibility of the production by pulsed electrodeposition of arrays with vertical or horizontal arrangement of nanoplates, layers of cone-shaped nanostructures as well as one-dimensional nanostructured arrays oriented perpendicular to the substrate surface without introducing of surfactant growth modifiers into electrolyte.

2. DESCRIPTION OF THE TEST OBJECT AND METHODS

Production of zinc oxide arrays was performed by the method of pulsed cathode electrochemical deposition in a three-electrode electrochemical cell with an aqueous electrolyte containing 0.01-0.05 M of $Zn(NO_3)_2$ and 0.1 M of $NaNO_3$. Glass plates covered by transparent electroconductive layers of fluorine-doped tin oxide (SnO_2:F or FTO) of Pilkington (USA) were used as the substrates (of cathodes or working electrodes). The surface area of the substrate-cathode covered by ZnO arrays was equal to 1 cm^2.

A platinum coil served as the counter electrode and a saturated silver-chloride Ag/AgCl electrode acted as the reference electrode. Pulsed electrodeposition modes of the investigated ZnO samples are given in Table 1. Mixing of the electrolyte during the electrodeposition of P48 and P49 samples was carried out using the magnetic stirrer MM-03; other samples were manufactured in stationary electrolytes. Temperature of the electrolytes t accounted for 60-70 °C. For the implementation of pulsed electrolysis, rectangular potential pulses were fed to the substrate-cathode using the pulse potentiostat PI-50-1.1 equipped by the programmer PR-8 that the lower limit of the cathode potential with respect to the reference electrode U_{off} was equal to – 0.8 V and the upper limit U_{on} was – 1.2 V or – 1.4 V (potentials are given relative to the reference electrode Ag/AgCl).

Thus, the amplitude of the cathode potential change at pulsed electrolysis was equal to 0.4 V or 0.6 V, respectively. The value of the assignable by the programmer working cycle (Dc, duty cycle) was calculated by the following formula:

$$Dc = T_{on}/(T_{on} + T_{off}) = T_{on} \cdot f, \quad (1)$$

where T_{on} is the time at the cathode potential U_{on}; T_{off} is the time at the cathode potential U_{off}; f is the frequency, i.e. the value inverse to the cycle time T_c:

$$f = 1/(T_{on} + T_{off}) = 1/T_c. \quad (2)$$

In electrodeposition of each separate sample during 10 or 60 min, frequency of pulses f remained constant.

Investigation of the optical properties of zinc oxide layers was performed using spectrophotometer SF-2000. FTO/glass substrates of Pilkington (USA) were used as the check samples in the registration of the optical transmission spectra $T(\lambda)$. Optical band gap E_g of zinc oxide layers was determined based on the correlation [16]:

$$\alpha = A \cdot (h\nu - E_g)^n / h\nu, \quad (3)$$

where α is the absorption coefficient of a semiconductor layer of the thickness d; $\alpha = -1/d \cdot \ln T$; A is the constant depending on the effective mass of charge carriers in the material; $h\nu$ is the energy of optical quanta; n is the exponent defined by the photon absorption mechanism in the semiconductor ($n = 1/2$ for the direct band semiconductor which ZnO is).

Since, for example, in the case of the formation of one-dimensional nanocrystals it was difficult to establish the exact thickness of the zinc oxide layer; E_g was determined by the extrapolation of a linear section of the dependence graph of $[(-\ln T) \cdot h\nu]^2$ on $h\nu$ on the energy axis.

A disorder of the structure of electrodeposited zinc oxide layers was estimated according to the work [16] by the value of the Urbach energy E_o proceeding from the fact that the absorption coefficient near the forbidden band is characterized by the exponential dependence on the photon energy:

$$\alpha = \alpha_0 \cdot \exp(h\nu/E_0), \quad (4)$$

where α_0 is the constant.

The value of the Urbach energy for electrodeposited arrays of zinc oxide was determined by the slope of a linear section of the dependence $\ln[-\ln T]$ on $h\nu$.

For the purpose of the analysis of the structural and substructural parameters of ZnO arrays, X-ray spectra (XRD) were registered using the diffractometer DRON-4M in CoK_α ($\lambda_{CoK\alpha} = 1.7889$ Å) or NiK_α ($\lambda_{NiK\alpha} = 1.65784$ Å) (sample P60) radiation. Scanning was performed in the Bragg-Brentano focusing (θ-2θ). Processing of the obtained X-ray diffraction patterns (background separation, $K_{\alpha1}$-$K_{\alpha2}$ doublet separation, etc.) as well as calculation of the parameters of diffraction line profile were carried out using "New_Profile v.3.4 (486)" and "OriginPro v.7.5" programs. Presence of crystal phases was revealed by comparison of the data of experimental X-ray diffraction patterns with the reference database JCPDS by using "PCPDFWIN v.1.30" program. Evaluation of coherent scattering regions (CSRs) and microstress values $\Delta d/d$ (where d is the lattice spacing according to JCPDS; Δd is the difference between the experimental and reference values of the lattice spacing) in ZnO arrays was performed by the analysis of the broadening of the X-ray diffraction maxima taking into account the instrumental broadening by the Williamson-Hall approximation method according to [17-19]. Parameters of the crystal lat-

Table 1 – Pulsed cathode electrodeposition modes and optical characteristics of nanostructured ZnO arrays

Sample	Electrolyte composition	Electrolyte mixing	U with respect to Ag/AgCl, V		t, °C	Electrodeposition time, min.	Frequency f, Hz	Dc	Optical characteristics		
			U_{off}	U_{on}					$T_{400\text{-}800}$, %	E_g, eV	E_o, eV
P18	$Zn(NO_3)_2$ – 0.05 M $NaNO_3$ – 0.1 M	–	– 0.8	– 1.4	70	60	200	0.4	16	3.11	0.50
P34		–	– 0.8	– 1.4	60	60	2	0.6	48	3.32	0.16
P35		–	– 0.8	– 1.4	68	60	2	0.4	55	3.39	0.15
P48		+	– 0.8	– 1.4	65	10	2	0.4	33,62,72	3.34	0.29
P49		+	– 0.8	– 1.4	70	10	2	0.4	35	3.37	0.19
P51		–	– 0.8	– 1.4	76	10	2	0.4	80	3.37	0.10
P60	$Zn(NO_3)_2$ – 0.01 M $NaNO_3$ – 0.1 M	–	– 0.8	– 1.4	70	10	2	0.4	66	3.21	0.41
P58		–	– 0.8	– 1.2	70	10	2	0.4	44	3.22	0.45

tice a and c of the zinc oxide hexagonal phase were calculated by the position of two last indexed lines of the X-ray diffraction patterns by the Nelson-Riley graphical extrapolation method and specified by the least square method (LSM) by means of "UnitCell" program using all registered reflections of the X-ray diffraction patterns in accordance with [17-19]. Residual stresses σ in zinc oxide arrays were calculated on the basis of the data on the lattice parameters of electrodeposited c and reference c_{bulk} (c_{bulk} = 5.207 Å) samples using the values of the elastic constants of the material in different directions according to [18]:

$$\sigma = -233 \cdot (c - c_{bulk}) / c_{bulk}. \quad (5)$$

For the investigation of the texture of electrodeposited zinc oxide arrays by the Harris method [19], we have used the values of the integral intensities of the X-ray diffraction peaks I_i. For each peak we calculated the value of the pole density P_i, which characterizes the probability that the normal to the crystallite surface coincides with the normal to the (hkil) plane, i.e. determines the number of crystallites, whose (hkil) planes are parallel to the sample surface, by the correlation [19]:

$$P_i = N \cdot (I_i / I_{0i}) \Big/ \sum_{i=1}^{N} I_i / I_{0i}\ , \quad (6)$$

where I_{0i} is the integral intensity of the i-th X-ray diffraction peak based on the JCPDS data; N is the number of X-ray diffraction peaks.

Pole densities were determined for all registered X-ray diffraction peaks; the value of $P_i > 1$ was ascribed to the texture axis.

Investigation of the surface morphology of zinc oxide arrays was carried out by the semi-contact method of the atomic force microscopy (AFM) on the plant "Nano-Laboratory Ntegra Prima NT-MDT".

3. DESCRIPTION AND ANALYSIS OF THE RESULTS

As the X-ray diffraction analysis of electrodeposited in pulsed mode zinc oxide layers has shown (Fig. 1), all of them are single-phase and have typical for the given material [1, 6] hexagonal ZnO structure of the wurtzite modification (JCPDS 36-1451). In Table 2 we present the structural and substructural characteristics of electrodeposited ZnO arrays. As it is seen from Fig. 1 and Table 2, all electrodeposited zinc oxide arrays were nanocrystalline (their CSRs did not exceed tens or one-two hundreds of nanometers), as a rule, were characterized by the increased lattice parameters compared with the reference ZnO (a = 3.250 Å, c = 5.207 Å according to JCPDS 36-1451), as well as insignificant microstresses $\Delta d/d$ and residual compression stresses σ. At the same time, differences in the sample texture were significant and texture, as known [1, 5-13], is closely connected with the morphology of nanostructured zinc oxide arrays. As it was pointed in [6], (0002) texture is typical for ZnO with the wurtzite structure, i.e. growth of polar planes with high energy formed by Zn^{2+} and O^{2-}, which belong to ± (0001) family, along the c axis. (0002) texture is explained by the fact that during the formation of new ZnO nuclei, precursors Zn^{2+} and OH^- in the equilibrium conditions are mainly adsorbed on polar planes with the opposite charge. Due to this fact, one can observe a fast crystallite growth in the <0001> direction in comparison with the growing of their non-polar planes, for example, $\{1\bar{1}00\}$ and $\{2\bar{1}\bar{1}0\}$. Thus, 1D nanostructures are formed. The authors of [1] indicate that in the conditions of electrochemical deposition, in the cases, when mass transfer of zinc ions is a slower stage compared with the generation of hydroxyl groups on account of the reduction of nitrate-ions and water, diffusion of Zn^{2+} limits the process of ZnO formation providing the formation of one-dimensional nanostructures of this material in the form of extended hexagonal prisms with the c axis oriented perpendicular to the substrate. If diffusion (Zn^{2+}) and ion generation (OH^-) rates are of the same order of magnitude, then thickened ZnO nanorods are formed, since growth occurs both along the longitudinal c axis and in the transverse directions. At very large diffusion rates, for example, in concentrated solutions of zinc salts, continuous films of zinc oxide are formed. The authors of [1] have also shown that in the conditions of blocking of the formed Zn^{2+} positively charged planes from the (0001) family, for example, due to the specific adsorption of negatively charged chloride-ions, growth of ZnO in the direction $(10\bar{1}0)$ in the form of arrays of hexahedral nanoplates, whose lateral surface is perpendicular to the substrate, becomes preferential.

Pulsed electrochemical deposition allowed to affect the preferred orientation of nanocrystalline ZnO arrays

Table 2 – Structural and substructural characteristics of electrodeposited ZnO arrays

Sample	CSR, nm	Microstress $\Delta d/d \cdot 10^3$	Residual stress σ, GPa	Lattice parameter, Å				Texture	
				Nelson-Riley method		LSM		Pole density P_{hkl}	$h\ k\ i\ l$
				a	c	a	c		
P18	20-70	6.4-7.9	0.18	3.265	5.179	3.260	5.202	2.01 1.45	(0002) $(10\bar{1}\,3)$
P34	40-80	0.4-1.6	− 0.49	3.256	5.219	3.257	5.217	1.90 1.71 1.07	$(10\bar{1}\,2)$ $(10\bar{1}\,3)$ (0002)
P35	70-200	0.7-1.7	− 0.45	3.256	5.223	3.257	5.216	6.24	(0002)
P48	30-50	0.2-3.5	− 0.22	3.249	5,203	3.255	5.211	2.80 1.98	$(10\bar{1}\,0)$ $(11\bar{2}\,0)$
P49	70-200	0.6-1.5	− 0.67	3.248	5.225	3.255	5.221	3.89 1.00 1.00	(0002) $(10\bar{1}\,2)$ $(10\bar{1}\,3)$
P51	110-200	0.6-1.4	− 0.40	3.249	5.225	3.252	5.215	4.24 1.28 1.10	(0002) $(10\bar{1}\,3)$ $(20\bar{2}\,1)$
P60	40-60	0.2-1.9	− 0.36	3.249	5.221	3.251	5.214	3.62	(0002)
P58	60-140	0.6-1.4	− 0.18	3.252	5.208	3.253	5.210	2.29 1.36 1.23	$(10\bar{1}\,3)$ $(10\bar{1}\,2)$ (0002)

because of the change in the pulse duration and pauses T_{on} and T_{off}, respectively, i.e. by variation of the pulse frequency f and working cycles D_c. As we have earlier described in the work [7], based on the thermodynamic restrictions on the electrochemical deposition processes, only those electrochemical reactions can occur on the cathode, whose standard potential E^0 is more positive than the cathode potential U; therefore, during the pause T_{off}, i.e. at $U_{off} = -0.8$ V, ions NO_3^- and Zn^{2+} diffuse to the cathode for the formation of ZnO on its surface as a result of the interaction of zinc ions and hydroxyl groups by the reactions (7)-(10):

$$NO_3^- + H_2O + 2\bar{e} \rightarrow NO_2^- + 2OH^-,\ E^0 = -0.21\ \text{B}, \quad (7)$$

$$NO_3^- + 2H_2O + 3\bar{e} \rightarrow NO\uparrow + 4OH^-,\ E^0 = -0.36\ \text{B}, \quad (8)$$

$$NO_3^- + 7H_2O + 8\bar{e} \rightarrow NH_4OH + 9OH^-,\ E^0 = -0.34\ \text{B}, \quad (9)$$

$$Zn^{2+} + 2OH^- \rightarrow Zn(OH)_2 \rightarrow ZnO + H_2O. \quad (10)$$

During the potential pulse T_{on}, i.e. at $U_{on} = -1.4$ V, in addition to the reactions (6)-(10), formation of hydroxyl groups by the reactions (11), (12) also takes place:

$$NO_3^- + H_2O + \bar{e} \rightarrow NO_2\uparrow + 2OH^-,\quad E^0 = -1.05\ \text{B}, \quad (11)$$

$$2H_2O + 2\bar{e} \rightarrow H_2\uparrow + 2OH^-,\quad E^0 = -1.05\ \text{B}; \quad (12)$$

moreover, cathodic reduction of zinc occurs according to the reaction:

$$Zn^{2+} + 2\bar{e} \rightarrow Zn,\quad E^0 = -0.98\ \text{B}, \quad (13)$$

which is followed by the heterogeneous chemical reaction during the next pause (at U_{off})^

$$Zn + NO_3^- + H_2O \rightarrow NO_2^- + Zn(OH)_2 \rightarrow NO_2^- + ZnO + H_2O. \quad (14)$$

As a result, during the pulsed electrolysis the rate of rise of zinc oxide arrays increases compared with direct-current electrodeposition. Moreover, at high frequencies f and relatively long-term pulses (at large working cycles Dc), significant deviations of the ZnO formation process from the equilibrium one are observed. In Fig. 2 we illustrate the images, obtained by the atomic force microscopy (AFM) method, of the surface of the produced at increased frequency $f = 200$ Hz sample P18 (Fig. 2a); electrodeposited at increased working cycle ($Dc = 0.6$) sample P34 (Fig. 2b) and obtained at small frequency $f = 2$ Hz and shorter working cycle ($Dc = 0.4$) sample P35 (Fig. 2c) with typical one-dimensional preferential growth perpendicular to the substrate surface, to which perfect texture of this sample corresponds $P_{(0002)} = 6.2$ corresponds (Table 2). Shape of the presented in Fig. 2a ZnO arrays in the form of regular hexagonal nanoplates, to our opinion, is explained by the fact that in the case of pulsed electrolysis, the charge-discharge process of a double electric layer (capacitive process) takes place on the cathode along with the process of electrochemical reduction (Faraday process) [21]. Based on the data of the work [21], influence of the capacitive process is exhibited in the shape distortion and decrease in the pulse amplitude with increasing their frequency. As it turned out, increase in the pulse frequency of the cathode potential to $f = 200$ Hz leads to the increased impact of the capacitive process resulting in decreasing the generation of hydroxyl groups on the cathode; it becomes comparable with the diffusion rate of Zn^{2+} that is exhibited on the structure and properties of zinc oxide arrays in the growth inhibition of the (0002) plane, and, therefore, in

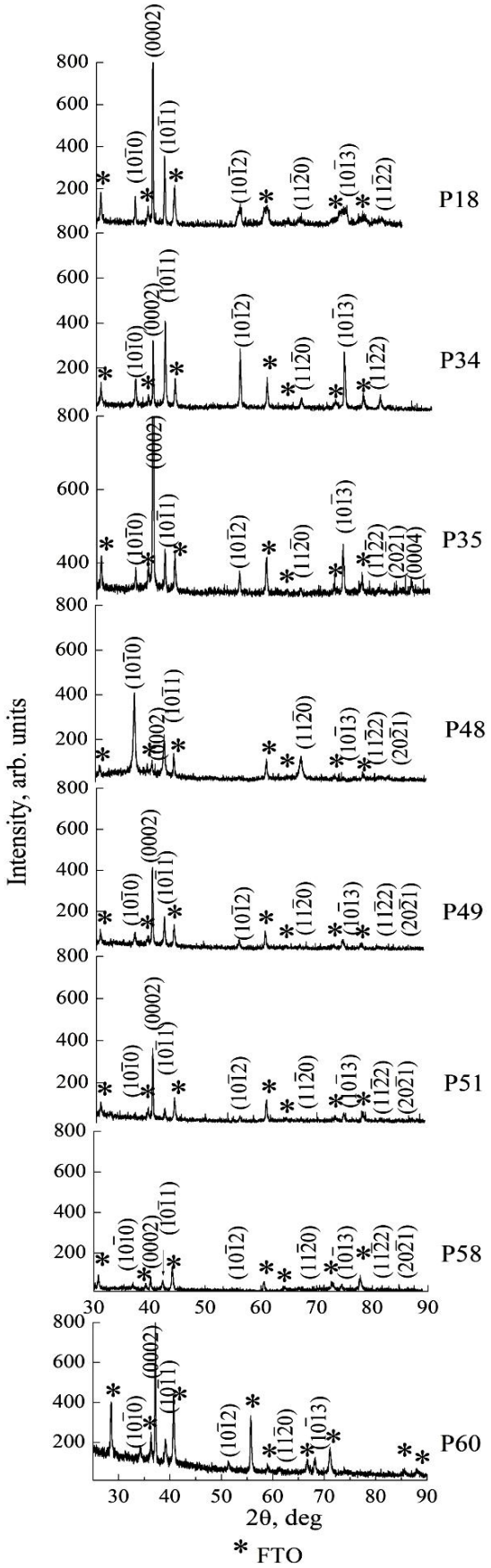

Fig. 1 – X-ray diffraction patterns of the nanosized zinc oxide arrays electrodeposited on the FTO/glass substrates

the decrease in the texture perfectness along the <0001> direction. Sample P18 shown in Fig. 2a has two weak preferred orientations: $P_{(0002)} = 2.01$ and $P_{(10\bar{1}3)} = 1.45$ (Fig. 1, Table 2).

Demonstrated in Fig. 2b stacks of hexagonal nanoplates, whose lateral surfaces are oriented perpendicular to the substrate plane, are similar in external view to the ZnO nanostructures shown in the works [1, 6] and grown by different liquid-phase methods at a specific adsorption of surfactants.

Probably, at $Dc = 0.6$, i.e. when the pulse duration exceeds the pause duration, bubbles of hydrogen, which is formed according to the reaction (12), are adsorbed on the surface of the growing ZnO crystal especially on the planes of the (0001) family at $U_{on} = -1.4$ V. Since pulsed electrochemical process has a periodic behavior, one observes periodicity in the ZnO growth mechanisms, because of what nanostructured arrays in Fig. 2b has the form of a set of stacks of hexagonal plates, whose lateral surfaces are oriented to the substrates. As seen from Table 2, sample P34 to an almost equal degree is textured in two directions: $P_{(10\bar{1}2)} = 1.90$, $P_{(10\bar{1}3)} = 1.71$.

We have proved earlier in [7-8, 11, 20] that for the preferential growth of zinc oxide arrays of the wurtzite modification in the direction perpendicular to the substrate surface, i.e. along the *c* axis, it is necessary to eliminate adsorption on the (0002) surface of gaseous substances, in particular, of hydrogen bubbles formed during the electrochemical cathode deposition of ZnO. The authors of the works [7-8, 11, 20] using X-ray diffraction investigations succeeded to demonstrate that frequency of the potential pulses $f = 2$ Hz corresponds to these requirements. This frequency favors electrodeposition of zinc oxide arrays with a perfect texture in the <0001> direction that is probably connected with fast desorption of gaseous reaction products in electrodeposition of ZnO arrays. On the other hand, electrochemical and diffusion stages during electrochemical growing of zinc oxide arrays in the pulse mode are governed by the working cycle *Dc* by controlling the durations T_{on} and T_{off}. Our investigations [7-8, 11, 20] have shown that 1D nanostructured ZnO arrays can be formed only at $Dc = 0.40$ that is confirmed by Fig. 2.

Optical investigations of nanostructured ZnO arrays electrodeposited in different pulse modes (Table 1, Fig. 3) have revealed that transparency in the visible range is higher for the samples with perfect texture (0002). The optical band gap E_g corresponds to the value for a bulk zinc oxide ($E_{gbulk} = 3.36$ eV). Sample P18 produced at increased frequency is characterized by significantly lower value $E_g = 3.11$ eV, probably, due to its structural disordering (the smallest CSR of 20-70 nm and the largest Urbach energy of $E_0 = 0.5$ eV).

Tables 1, 2, as well as Fig. 4, demonstrate that with decreasing duration of the electrodeposition process in the conditions optimal for the formation of one-dimensional ZnO nanostructures ($Dc = 0.40$, $f = 2$ Hz), more transparent layers of shortened 1D nanorods with the (0002) texture are formed (sample P51, Fig. 4a).

As our investigations on the modification of mass transfer process during pulsed electrodeposition of ZnO on account of convection have shown, mixing of electro-

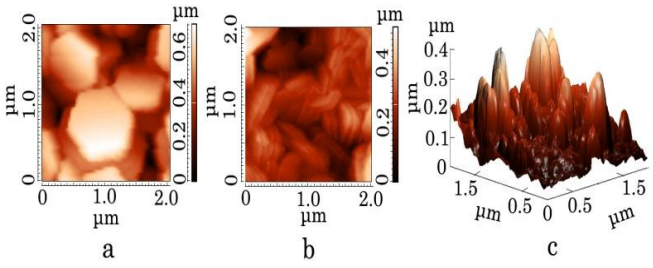

Fig. 2 – AFM-images of the surface of nanostructured ZnO arrays: P18 (a), P34 (b), P35 (c)

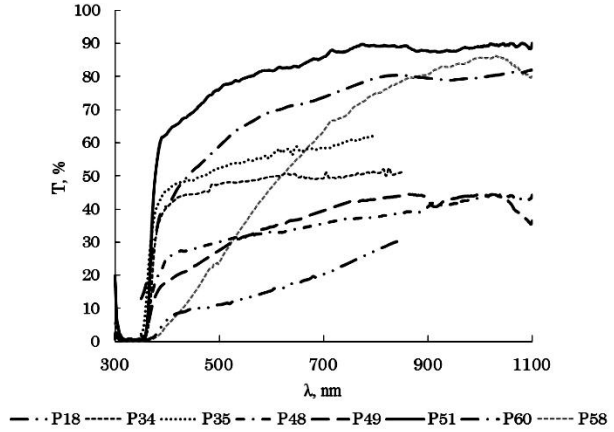

Fig. 3 – Optical transmission spectra of nanostructured ZnO arrays electrodeposited in different pulse modes

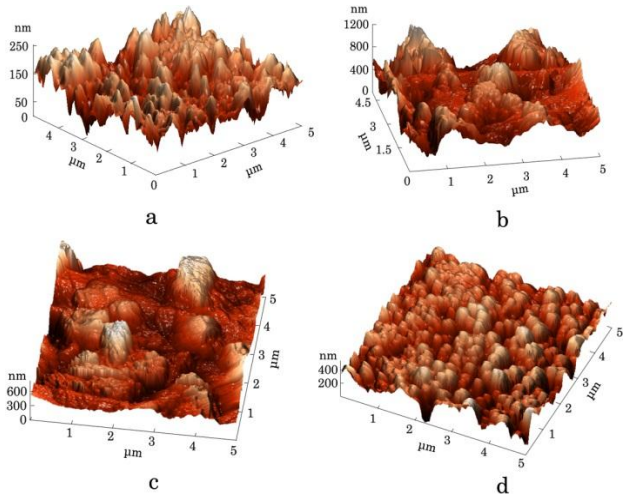

Fig. 4 – AFM-images of the surface of nanostructured ZnO arrays: P51 (a), P48 (b), P49 (c), P58 (d)

lyte has a disordering effect on the growth of nanosized ZnO arrays which is exhibited in the decrease of the CSR, increase in the residual stresses, attenuation of the array texturing in the <0001> direction, decrease in the transparency in the visible range and increase in the Urbach energy. Samples P48 and P49 electrodeposited using mixing of electrolyte by a magnetic stirrer were characterized by the irregularity of the substrate surface coating. In Table 1 we present 3 values of $T_{400\text{-}800}$ for the sample P48 measured on its different sections. In Fig. 4b, c we show the morphology of nanostructured ZnO arrays electrodeposited in the conditions of the convective mass transfer which demonstrates nanolevel nonuniformity of ZnO layers.

To our opinion, the negative impact of electrolyte convection on the nanostructure morphology is explained by very fast and, the chief, irregular inflow of zinc ions to the ZnO growth surface on the cathode-substrate that leads to the order inversion of this growth.

Decrease in the concentration of zinc salt $Zn(NO_3)_2$ in electrolyte from 0.05 M to 0.01 M naturally slowed down diffusion of Zn^{2+} in comparison with generation of OH^- on the cathode; the process became more equilibrium, therefore, at $Dc = 0.4$ and $f = 2$ Hz nanostructured 1D zinc oxide arrays were formed. These arrays consisted of elongated hexagonal prisms oriented perpendicular to the substrate surface and had the $P_{(0002)} = 3.6$ structure (sample P60 in Fig. 1 and Table 2). Decrease in the value of the pulse potential to $U_{on} = -1.2$ V at $Dc = 0.4$ and $f = 2$ Hz (sample P58) maintained the upward trend of 1D ZnO nanostructures, however, the tips of the nanorods oriented perpendicular to the substrate have lost the form of hexagonal prisms taking the form close to the cone-shaped (Fig. 4d) that was detected by X-ray diffraction analysis as the weakening of the (0002) texture. Decrease in U_{on} to − 1.2 V and simultaneous decrease in the amplitude of the potential change during pulsed electrodeposition of the sample P58 led, in addition, to the thinning of ZnO layer, i.e. to the decrease in the height of 1D nanostructures and a parabolic shape, to what the decrease in the intensity of all ZnO peaks on the XRD corresponds (Fig. 1).

In Fig. 3 we show the atypical optical transmission spectrum of the sample P58. We note that in the work [10] we have demonstrated for the first time the possibility to create by the method of pulsed electrochemical deposition from aqueous electrolytes of nanosized zinc oxide arrays with a parabolic salience profile.

4. CONCLUSIONS

In this work we have analyzed the reasons of the formation by pulsed cathode electrodeposition of ZnO arrays consisting of regular hexagonal nanoplates and their stacks with vertical or horizontal arrangement relative to the substrates, layers of parabolic ZnO nanostructures and also one-dimensional zinc oxide arrays oriented perpendicular to the substrate without using of surfactant growth modifiers in electrolyte. By atomic force microscopy method we have demonstrated the production of the specified nanostructured zinc oxide arrays. By means of X-ray diffractometry and optical spectroscopy we have studied the crystal structure and properties of zinc oxide arrays manufactured by the method of pulsed electrochemical deposition.

REFERENCES

1. M. Skompska, K. Zarębska, *Electrochim. Acta* **127**, 467 (2014).
2. Y.-C. Chao, C.-Y. Chen, C.-A. Lin, Y.-A. Dai, J.-H. He, *J. Mater. Chem.* **20**, 8134 (2010).
3. C. Battaglia, J. Escarré, K. Söderström, M. Charrière, M. Despeisse, F.-J. Haug, C. Ballif, *Nat. Photonics* **5**, 535

(2011).
4. J. Huang, Q. Wan, *Sensors* **9**, 9903 (2009).
5. A. Arslan, E. Hür, S. Ilican, Y. Caglar, M. Caglar, *Spectrochim. Acta A* **128**, 716 (2014).
6. S. Xu, Z.L., *Nano Res.* **4** No11, 1013 (2011).
7. N.P. Klochko, G.S. Khrypunov, Yu.O. Myagchenko, E.E. Melnychuk, V.R. Kopach, E.S. Klepikova, V.M. Lyubov, and A.V. Kopach, *Semiconductors* **46** No6, 825 (2012).
8. N.P. Klochko, G.S. Khrypunov, Y.O. Myagchenko, E.E. Melnychuk, V.R. Kopach, E.S. Klepikova, V.M. Lyubov, A.V. Kopach, *Functional Mater.* **19** No2, 276 (2012).
9. V.-M. Guérin, J. Rathousky, Th. Pauporté, *Sol. Energ. Mater. Sol. C* **102**, 8 (2012).
10. N.P. Klochko, G.S. Khrypunov, Y.O. Myagchenko, E.E. Melnychuk, V.R. Kopach, K.S. Klepikova, V.M. Lyubov, A.V. Kopach, *Semiconductors* **48** No4, 531 (2014).
11. N.P. Klochko, Y.O. Myagchenko, E.E. Melnychuk, V.R. Kopach, E.S. Klepikova, V.N. Lyubov, G.S. Khrypunov, A.V. Kopach, *Semiconductors* **47** No8, 1123 (2013).
12. P. Yang, H. Yan, S. Mao, R. Russo, J. Johnson, R. Saykally, N. Morris, J. Pham, R. He, H.-J. Choi, *Functional Materials* **12** No5, 323 (2002).
13. D. Dimova-Malnovska, P. Andreeva, M. Sendova-Vassileva, H. Nicheva, K. Starbova, *Energ. Procedia* **2**, 55 (2010).
14. K. Nomura, N. Shibata, M. Maeda, *J. Cryst. Growth* **235**, 224 (2002).
15. A. Goux, T. Pauporte, J. Chivot, D. Lincot, *Electrochim. Acta* **50**, 2239 (2005).
16. N. Shakti, P.S. Gupta, *Appl. Phys. Res.* **2**, 19 (2010).
17. S.S. Gorelik, L.N. Rastorguev, Yu.A. Skakov, *Rentgenograficheskii i elektronnoopticheskii analiz* (M.: Metallurgiya: 1970).
18. S.V. Tsybulya, S.V. Cherepanova, *Vvedenie v strukturnyi analiz nanokristallov: Ucheb. posobie* (Novosibirsk: NGU: 2008).
19. *Struktura i fizicheskie svojstva tverdogo tela. Laboratornyi praktikum: Ucheb. posobie* (Red. prof. d-ra fiz.-mat. nauk L.S. Palatnik) (K.: Vyshcha shkola: 1983).
20. G. Khrypunov, N. Klochko, N. Volkova, V. Kopach, V. Lyubov, K. Klepikova, *World Renewable Energy Congress (WREC 2011)*, 2853 (Linköping: Linköping University Electronic Press: 2011).
21. M.S. Chandrasekar, M. Pushpavanum *Electrochim. Acta* **53**, 3313 (2008).